

RelaMiX: Exploring Few-Shot Adaptation in Video-based Action Recognition

Kunyu Peng, Di Wen, David Schneider, Jiaming Zhang, Kailun Yang*, M. Saquib Sarfraz, Rainer Stiefelhagen, *Member, IEEE*, and Alina Roitberg, *Member, IEEE*

Abstract—Domain adaptation is essential for activity recognition to ensure accurate and robust performance across diverse environments, sensor types, and data sources. Unsupervised domain adaptation methods have been extensively studied, yet, they require large-scale unlabeled data from the target domain. In this work, we address *Few-Shot Domain Adaptation for video-based Activity Recognition (FSDA-AR)*, which leverages a very small amount of labeled target videos to achieve effective adaptation. This setting is attractive and promising for applications, as it requires recording and labeling only a few, or even a single example per class in the target domain, which often includes activities that are rare yet crucial to recognize. We construct FSDA-AR benchmarks using five established datasets considering diverse domain types: UCF101, HMDB51, EPIC-KITCHEN, Sims4Action, and ToyotaSmartHome. Our results demonstrate that FSDA-AR performs comparably to unsupervised domain adaptation with significantly fewer (yet labeled) target domain samples. We further propose a novel approach, RelaMiX, to better leverage the few labeled target domain samples as knowledge guidance. RelaMiX encompasses a temporal relational attention network with relation dropout, alongside a cross-domain information alignment mechanism. Furthermore, it integrates a mechanism for mixing features within a latent space by using the few-shot target domain samples. The proposed RelaMiX solution achieves state-of-the-art performance on all datasets within the FSDA-AR benchmark. To encourage future research of few-shot domain adaptation for video-based activity recognition, our benchmarks and source code are made publicly available at <https://github.com/KPeng9510/RelaMiX>.

Index Terms—Few-shot domain adaptation, action recognition, relation-based temporal aggregation, video classification.

I. INTRODUCTION

DOMAIN shifts, *i.e.*, distribution discrepancies between the source domain data and the target domain data, are inevitable in real-world applications, and the performance of human activity recognition models is strongly affected by, *e.g.*, changes in sensor types and -placements, different room layouts or transitions from synthetic to real examples [1], [2].

The vast majority of existing domain adaptation research concentrates on the Unsupervised Domain Adaptation

K. Peng, D. Schneider, J. Zhang, M. S. Sarfraz, and R. Stiefelhagen are with the Institute for Robotics and Anthropomatics, Karlsruhe Institute of Technology, Karlsruhe, Germany (email: firstname.lastname@kit.edu).

D. Wen is with the Institute for Robotics and Anthropomatics, Karlsruhe Institute of Technology, Karlsruhe, Germany (email: di.wen@student.kit.edu).

K. Yang is with the School of Robotics and the National Engineering Research Center of Robot Visual Perception and Control Technology, Hunan University, Changsha, China (email: kailun.yang@hnu.edu.cn).

M. S. Sarfraz is also with Mercedes-Benz Tech Innovation, Stuttgart, Germany.

A. Roitberg is with the University of Stuttgart, Stuttgart, Germany (email: alina.roitberg@f05.uni-stuttgart.de).

*Corresponding author: Kailun Yang.

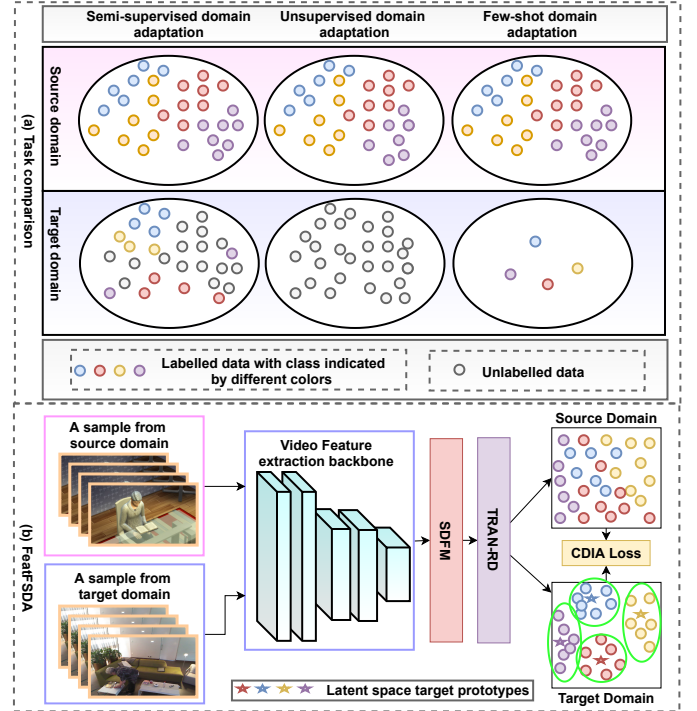


Fig. 1: (a) Comparison of the Semi-Supervised Domain Adaptation (SSDA), Unsupervised Domain Adaptation (UDA), and Few-Shot Domain Adaptation (FSDA) tasks. (b) An overview of our proposed RelaMiX approach.

(UDA) [3], [4], [5], [6], [7], [8], [9], and Semi-Supervised Domain Adaptation (SSDA) settings [10], [11], [12], [13]. These paradigms allow transferring the recognition ability from the source domain to the target domain. The benefit of unsupervised domain adaptation lies in the reduction of labor-intensive labeling tasks for large-scale data in the target domain. However, as shown in Figure 1(a), unsupervised domain adaptation and semi-supervised domain adaptation paradigms both require a substantial amount of samples from the target domain, whereas semi-supervised domain adaptation further demands a few labels from the target domain.

To address this drawback, we take a step towards the mostly uncharted area of **Few-Shot Domain Adaptation for Action Recognition (FSDA-AR)** illustrated in Figure 1(a). Instead of relying on a large number of examples from the target domain, FSDA-AR necessitates a minimal amount of labeled samples, *i.e.*, requiring only a few or even a single annotated sample per class in the target domain. These labeled target domain

samples serve as knowledge support to reduce the domain gap. Unlike pixel-wise tasks, *e.g.*, semantic segmentation [14], human activity recognition only requires a single label assigned to a video sample. Consequently, annotating a few target domain samples for the FSDA-AR is less time-consuming, since collecting more video data entails a lot of human effort to serve as actors or do video surveillance. The data collection of video samples needs quite a lot of data processing, few-shot domain adaptation is, therefore, more feasible. Despite this advantage, little research has been performed on FSDA-AR, so far. Of the published works most related to our tasks, one targets FSDA-AR in videos but the benchmark is not made available [15], whereas another work [16] tackles only a specific data type (radar-based activity recognition) that is not well-suited for general activity recognition. Xu *et al.* [17] focus on the FSDA on daily life and sports activities separately, while the feature extraction backbone is not as unified as in the UDA task, and more diverse domain shifts are not considered.

To further explore the applicability of FSDA-AR in more diverse and challenging domain adaptation settings, we employ an evaluation procedure involving five publicly available video-based human activity recognition datasets in our investigation. In order to investigate FSDA-AR under varying conditions, encompassing scenarios with both small and large domain gaps, we examine the adaptation from Sims4Action [2] to ToyotaSmartHome (TSH) [18], EPIC-KITCHEN [1], HMDB [19] to UCF [20], and UCF [20] to HMDB [19]. The selection of benchmarks in our study covers a spectrum of scenarios, including the evaluation of transfer learning between real-world activity recognition datasets exhibiting a small domain gap. Additionally, our investigation addresses the adaptation towards diverse domain gaps. In this benchmark, we include various approaches as baselines, *e.g.*, UDA approaches, few-shot activity recognition approaches, and statistic approaches, which are all reformulated into FSDA-AR settings accordingly.

In light of our observations, it has become evident that existing baselines are often incapable of providing consistent performance across the broad spectrum of domains inherent in the FSDA-AR task. To address this limitation, there is a pressing need for a novel method tailored specifically to few-shot domain adaptation, one that demonstrates resilience and adaptability to the diverse array of domains encountered in this context. Consequently, we introduce our novel approach for FSDA-AR in this study. The framework of our approach is guided by three fundamental objectives: (1) Enhancing temporal data generalization: Our primary goal is to augment the capacity of the model to generalize effectively when dealing with temporal data. This involves developing mechanisms that facilitate the extraction of temporal patterns and features that are transferrable across different domains. (2) Leveraging statistical distributions: We aim to capitalize on the statistical properties of source-domain samples while effectively utilizing a small number of labeled target-domain samples to enable feature blending within the latent space, thereby enhancing the model’s capacity for robust and discriminative feature learning. (3) Establishing a unified embedding space: We strive to create a shared embedding space that harmoniously integrates both

the source and target domains. This integrated space will enable the model to operate cohesively across the various domains, promoting cross-domain knowledge transfer.

To achieve these objectives, RelaMiX is proposed and its overview is provided in Figure 1(b). In our initial endeavor, we introduce a novel Temporal Aggregation Network designed to amplify the generalizability of acquired temporal features. This network, termed the Temporal Relational Attention Network with Relation Dropout (TRAN-RD), is purpose-built to capture more nuanced neighborhood information by considering diverse snippet levels, relational attention, and relation combinations, with relation dropout enforced to enhance the representativeness of each relation combination. Our second innovation centers on a Statistical Distribution-based Feature Mixture (SDFM) mechanism. This mechanism serves to augment the diversity of features within the aligned latent space. By computing the covariance and empirical mean for each temporal snippet, we construct Gaussian distributions for latent space features originating from the source domain. We subsequently generate mixed-domain features by employing empirical mean transformations and interpolation techniques. During training, we concurrently fine-tune the temporal aggregation network using features from both the source and target domains, as well as mixed features, fostering cross-domain knowledge transfer. Lastly, we introduce a Cross-Domain Information Alignment (CDIA) mechanism. This mechanism is instrumental in aligning source domain features in proximity to batch-wise centers in the target domain, while simultaneously distancing them from randomly selected negative anchors within the dataset. A similar alignment strategy is applied to the mixed features, drawing them closer to their temporally augmented positive anchors and away from randomly selected mixed features. This strategic approach effectively bridges the domain gap, facilitating robust feature transfer and domain adaptation by leveraging few-shot samples within our model.

These innovations address the challenge of leveraging diverse temporal information sources, promoting feature diversity, and facilitating effective domain alignment in a scientific and principled manner. RelaMiX therefore yields state-of-the-art performance on the established benchmark. Our contributions are summarized as follows:

- We explore the under-researched task of Few-Shot Domain Adaptation for Activity Recognition (FSDA-AR) by formalizing a new benchmark on five established datasets with diverse domains, including movie data to real-world third-person data, cross-person egocentric perspectives, as well as synthetic data to real data.
- We propose the new RelaMiX approach, consisting of three key components: a Temporal Relational Attention Network with Relational Dropout (TRAN-RD) to improve temporal generalizability, a Statistic Distribution-based Feature Mixing (SDFM) to augment the shared latent space, and Cross-Domain Information Alignment (CDIA) to bridge the challenging domain gaps.
- Our approach achieves state-of-the-art results on the FSDA-AR benchmark considering the 1-, 5-, 10-, 20-shot settings. Compared with UDA solutions, RelaMiX for FSDA-AR reaches comparable performance.

II. RELATED WORK

In this section, we present an overview of related work in two major areas: domain adaptation and activity recognition.

Domain Adaptation (DA). Domain Adaptation (DA) [3], [4], [5], [15], [21], [22], [23], [17] refers to a situation in which training and test data come from two domains that are related, but distinct from one another. Adapting a learner to a target domain is the goal of DA. Unsupervised Domain Adaptation (UDA) aims to solve this problem of inter-domain discrepancy without labeling target domain samples in training. Image-based tasks have been widely proposed using UDA methods [7], [21], [22], [24]. DAN [25] and JAN [26] put forward to align the marginal distributions of the source and target domains in the feature space by minimizing Maximum Mean Discrepancy (MMD) and Joint Maximum Mean Discrepancy (JMMD), respectively. For the video-based UDA, several existing works use an adversarial learning framework to deal with the domain shifts [3], [27]. Apart from adversarial learning, Wei *et al.* [4] adopt disentanglement learning to decouple the content and context information to achieve a better adaptation. CoMix [5] uses mixture techniques to introduce the background information from the target domain into the samples of the source domain during the training procedure to reduce the domain shift. Besides, recent research works in Semi-Supervised Domain Adaptation (SSDA) [10], [11], [12], [13], [28] relax the strict constraint of UDA by using a partially annotated target domain training set.

In Few-Shot Domain Adaptation (FSDA) [17], [29], [30], [31], [32], only a few labeled samples per class are given to formulate the target domain training set. Note that FSDA-AR does not rely on a large-scale unlabeled training set from the target domain to achieve the domain adaptation, while SSDA needs a large amount of the unlabeled data from the target domain. Yet, the research of Few-Shot Domain Adaptation in the field of video-based Activity Recognition (FSDA-AR) has been very limited with only three works targeting this task [15], [16], [17]. PASTN [15] uses an attentive adversarial network to learn domain-invariant features. FS-ADA [16] integrates both the category classifier and the domain discriminator to extract domain-invariant and category-discriminative features. Xu *et al.* [17] use the Timesformer [33] as the backbone and utilize prototype-based snippets contrastive learning to achieve FSDA-AR.

However, the benchmark of PASTN [15] is not available, the datasets used by Xu *et al.* [17] do not encompass different levels of the domain shift, and the feature extraction backbone is not unified as the same backbone, *e.g.*, I3D [34], which is widely used in UDA. Besides, FS-ADA [16] is developed for radar data. In this regard, we consider that a fair comparison should be conducted with UDA approaches reformulated in the FSDA-AR task for the adaptation against diverse domain shifts. Moreover, there is a strong need for further research of video-based FSDA-AR on diverse domain shifts, *e.g.*, different views of egocentric videos and synthesized videos to real videos, taking into account the unification of the feature extraction backbone to make fair task comparison with UDA and the existing works in the FSDA-AR field. To address this

issue, we introduce a novel video-based FSDA-AR benchmark with diverse domain combinations and under the unification of the feature extraction backbone.

We further propose the RelaMiX approach, which uses three key components to increase the generalization of video data. A temporal relational attention network with relation dropout is used to improve the generalizability of the learned temporal relational embeddings. Statistic distribution-based feature mixture is used to enhance the diversity of the learned latent space in terms of the target domain, which is inspired by the work from Yang *et al.* [35], designed for image-based few-shot learning for feature generation. Finally, we use cross-domain information alignment to bridge the gap between the source domain and target domain by using contrastive supervision using mixed domain negative anchors and prototype-based positive anchors. Our method shows promising performance across five different datasets for the FSDA-AR task.

Video-based Human Activity Recognition (HAR). Supervised human activity recognition methods [36], [37], [38], [34], [39], [40], [41] have achieved impressive results with deep learning algorithms in recent years. The video-based approaches can be grouped into Convolutional Neural Networks (CNNs) based and transformer-based methods. For CNN-based methods, most of the existing approaches leverage 3D CNNs and diverse temporal aggregation techniques. TSN [37] samples a fixed number of video frames evenly across the video segments, and uses these sampled frames as input for a two-stream network. I3D [34] uses an inflated Inception v1 model [42] with 3D convolutional layers utilized in each stage. S3D [39] decomposes the lower 3D convolutional layers of I3D into two separate operations, a spatial and temporal convolution convolution. X3D [40] expands a tiny base 2D image architecture into a spatiotemporal one by expanding multiple possible axes in space, time, channels, and depth. As a result, an optimal trade-off is achieved between accuracy and complexity. Another group of network architectures leverages transformer-based backbones [43], [33], [44]. Most of existing UDA works [3], [4], [5], [27] make use of I3D [34] or ResNet [45] as the feature extractor.

Following the standard setting of UDA [3], [4], [5], [27], we leverage I3D [34] as our feature extractor in the proposed RelaMiX method, allowing adequate comparison between the FSDA-AR and UDA tasks. To enable domain generalizable feature learning, our RelaMiX incorporates generalizable temporal-relation-based aggregation, source domain statistics-based feature mixture, and cross-domain information alignment supervision, which enable RelaMiX to elevate state-of-the-art performances on the FSDA-AR benchmark.

III. METHOD

A. Problem Formulation

Comparison with Other Domain Adaptation Settings. We begin by distinguishing the few-shot domain adaptation task from other domain adaptation settings commonly used in previous research. The task we address is Few-Shot Domain Adaptation (FSDA), where a very small amount of labeled examples are available for each category in the target domain.

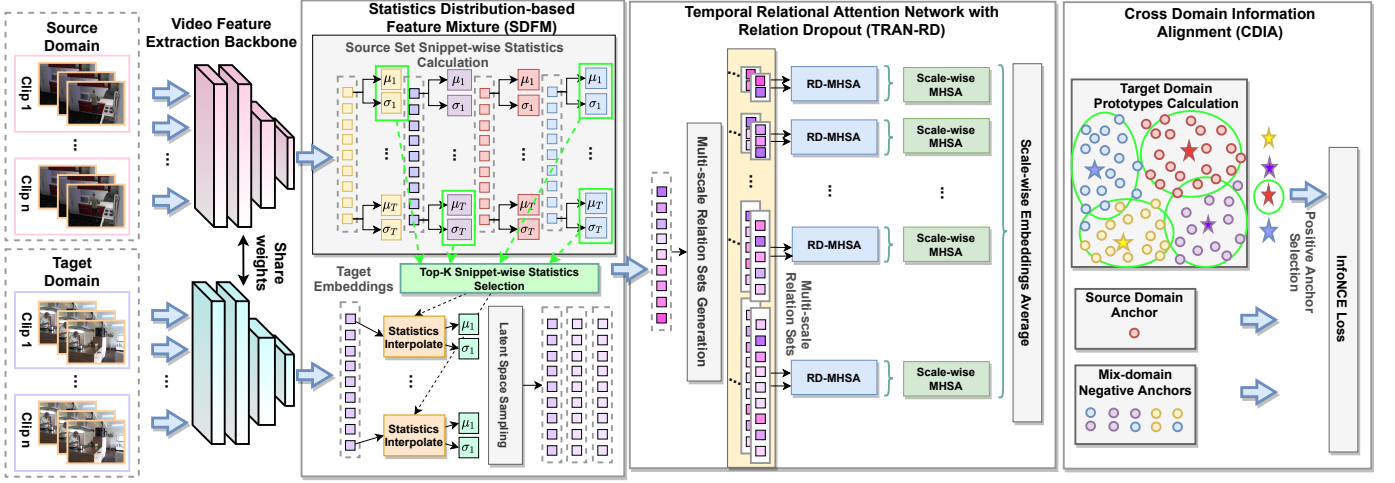


Fig. 2: An overview of the proposed RelaMiX framework. The input video is first separated into overlapped snippets extracted through a fixed-size temporal sliding window and then fed into the video feature extraction backbone to extract snippet-level features. Then, we calculate the statistical empirical mean and covariance of each class for each snippet considering all the samples from the source domain training set. The mean and covariance of the Top-K nearest centers corresponding to a snippet from the given query are chosen to generate the synthesized cluster center of the samples of target-domain latent space. We use the generated mean and covariance to formulate Gaussian distributions for each temporal snippet and sample more latent space features according to the few available shots from the target domain. Next, temporal relation sets are built, we make use of Relation-Dropout Multi-Head Self-Attention (RD-MSHA) to learn representative features within each relation set while using scale-wise Multi-Head Self-Attention (Scale-wise MSHA) to aggregate features across different relation scales. Finally, alongside cross-entropy losses, Cross-Domain Information Alignment (CDIA) loss is leveraged to bridge the domain gap by using target space batch-wise prototypes.

The comparison among the commonly addressed tasks of Semi-Supervised Domain Adaptation (SSDA) [10], [11], [12], [13], Unsupervised Domain Adaptation (UDA) [3], [4], [5], [7], [8], [9], and our FSDA is provided in Figure 1. In contrast to FSDA, both UDA and SSDA necessitate a large amount of unlabeled data in the target domain to construct the training set, while collecting such large-scale data with high quality might not be feasible in certain applications. FSDA, on the other hand, requires only a small number of labeled examples from the target domain, balancing the trade-off between data collection expenses and labeling efforts. In our benchmark, the leveraged few-shot setting results in a 70% to 98% reduction of data from the target domain to construct the training set compared to SSDA and UDA. Activity recognition does not rely on pixel-level dense annotation, which makes the trade-off between annotation and data collection considerable. It is crucial to note that FSDA is distinct from domain adaptation for few-shot learning [46], [47], which is specifically designed for adapting to new classes with limited examples, while we are adapting to new domains. FSDA does not encompass new activity classes.

Few-shot Domain Adaptation Formulation. The task we address assumes a fully labeled large-scale source domain training set $D_s = (v_i^s, l_i^s)_{i=1}^{N_s^{train}}$ and a small target domain training set $D_t = (v_i^t, l_i^t)_{i=1}^{N_t^{train}}$, which contains only few labeled samples per class. Our objective is to train a model using both D_s and D_t so that the resulting model performs well on the target domain test set, denoted as $T_t = (v_i^t, l_i^t)_{i=1}^{N_t^{test}}$. In

this context, N_s^{train} , N_t^{train} , and N_t^{test} represent the number of samples in the source domain training set, target domain training set, and target domain test set, respectively. The index of the sample is represented by i , while the video samples and corresponding labels are represented by v and l . The source and target domains are denoted by s and t , respectively.

B. Baselines on FSDA-AR Benchmark

We construct diverse baselines for our FSDA-AR benchmark by using three FSDA-AR approaches, *i.e.*, FS-ADA [16], SSA²Lign [17], and PASTN [15], established UDA approaches reformulated for FSDA-AR, *i.e.*, TA³N [3] and TranVAE [4], CoMix [5], and CO²A [27], few-shot human action recognition approaches reformulated for FSDA-AR, *i.e.*, TRX [48] and HyRSM [49], as well as the statistical baselines, *i.e.*, random chance (Random), K-Nearest Neighbors (KNN), Nearest Neighbor (NN), and Nearest Center (NC). For consistency, we use the I3D backbone [34] pre-trained on Kinetics400 [50] for all baselines, as I3D is commonly used for video feature extraction in UDA tasks [4].

Statistical Baselines. We first extract video features using I3D, discarding the last classification layer. All the statistical baselines (except for the Random baseline) are based on the extracted features. For the Random method, we randomly assign a class to a test set sample to establish the lower bound.

In the KNN method, we assign a label to a test set sample by averaging the performance of the 3-, 5-, and 10-NN methods, with neighbors selected from the source domain training set. For the Nearest Center method, we first calculate class centers

in the source domain training set and then assign the label of the nearest class center in the source domain to the target domain test set sample. In the Nearest Neighbor method, we assign the label of the nearest sample in the source domain training set to the sample from the target domain test set. Since these statistical baselines use the same source domain training set as support, the performance remains the same across different shot settings. These statistical baselines are used to showcase the Domain Generalization (DG) performance when no few-shot sample from the target domain is provided to better illustrate the benefits brought by the target domain few-shot samples.

Unsupervised Domain Adaptation (UDA) Baselines. To enrich our FSDA-AR benchmark and enable comparisons with the existing domain adaptation frameworks, we implement and restructure several established video-based UDA methods to suit the few-shot domain adaptation task. This is achieved by incorporating supervised classification loss on the target domain training set and converting the unsupervised contrastive loss into triplet margin loss where only few-shot samples from the target domain are provided. Specifically, we leverage four prominent methods: TA³N [3], TransVAE [4], CO²A [27], and CoMix [5], where TA³N and CO²A leverage domain adversarial learning, TransVAE concentrates on domain disentanglement, and CoMix targets at bridging the domain gaps by mixing the background information from both domains.

Few-shot Learning Baselines. Two representative works for video-based few-shot learning are leveraged, *i.e.*, TRX [48] and HyRSM [49], to test the performance of few-shot learning approaches in the few-shot domain adaptation task.

Few-shot Domain Adaptation (FSDA) Baselines. We employ three approaches from few-shot domain adaptation in the field of human activity recognition. The first approach is FS-ADA [16], which targets radar-based FSDA using adversarial domain adaptation. The second approach is PASTN [15], which introduces a pairwise attentive, adversarial spatiotemporal network, and the third approach is SSA²Lign [17], which makes use of attentive alignment of snippets to bridge the domain gap. To explore FSDA-AR against more diverse domain shifts and achieve the unification of the feature backbone to keep a fair comparison with the UDA task, we establish a novel benchmark, using publicly accessible datasets encompassing diverse domain styles, and then replicate their performance by unifying the video extraction backbone as I3D [34] to provide a fair comparison with UDA methods.

C. Introduction of Our Proposed RelaMiX Method

In this section, we present the key ideas of our proposed RelaMiX approach (depicted in Figure 2). RelaMiX first uses I3D [34] to extract snippet-wise features. Then it incorporates a statistic distribution-based feature mixture approach to enrich the information in the latent space shared across domains, a temporal relation attention network with relation dropout to achieve more generalizable temporal information aggregation, and a cross-domain information alignment loss for representative feature learning to bridge the domain gap.

Snippet-wise Video Feature Extraction. Similarly to our baselines, we adopt I3D [34] as our backbone to obtain video

representations and a temporal sliding window to extract the snippet features for a given video. Let us consider a video sample represented as $\mathbf{v} = \{\mathbf{v}_1, \dots, \mathbf{v}_{N_T}\}$, where \mathbf{v}_i indicates the i th frame of the given video \mathbf{v} , N_w is the window size of the sliding temporal window and N_T is the number of the frames. We can obtain a set of video snippets, denoted as $\{\mathbf{s}_i\} = \{\{\mathbf{v}_i, \dots, \mathbf{v}_{i+N_w}\} \mid i \in [1, N_T]\}$ (zero padding is used at the start and end of the video). Next, we extract snippet-wise features. By inputting these snippets into the previously mentioned I3D-based feature extractor H_α , we can acquire the set of clip features for a sample as $\mathbf{f} = [H_\alpha(\mathbf{s}_1), \dots, H_\alpha(\mathbf{s}_{N_T})]$. **Statistic Distribution-based Feature Mixture (SDFM).** To better leverage the information provided by the few-shot samples from the target domain, we propose a new method, SDFM, to synthesize more target-domain embeddings by using the statistics calculated on the snippet features from the source domain training set. Next, the details of the SDFM will be illustrated. We first calculate the statistic centers and covariance matrix as Eq. 1.

$$\mu_c^t, \sigma_c^t = \frac{\sum_{i=1}^{N_c} \mathbf{f}_{(c,u)}^t}{N_c}, \sqrt{\frac{\sum_{i=1}^{N_c} (\mathbf{f}_{(c,i)}^t - \mu_c^t)^2}{N_c - 1}}, \quad (1)$$

where μ_c^t and σ_c^t indicate the mean and covariance of embeddings of the c th category and t th snippet from the source domain. N_c denotes the sample number for category c . $\mathbf{f}_{(c,j)}^t$ indicates the embeddings from the j th sample inside c th category considering the t th snippet.

Then, considering a sample provided by the few-shot target domain training set with embeddings $\hat{\mathbf{f}}$, we first calculate the Top-K nearest cluster centers for each snippet according to the distance to the mean of the snippet embeddings from the source domain for each temporal snippet individually, as depicted in Eq. 2.

$$I_c^t = \text{Top}K_{c \in \Omega_c} (e^{(1-D(\mu_c^t, \hat{\mathbf{f}}^t))}), \quad (2)$$

where I_c^t indicates the categories which are selected. $D(\cdot)$ indicates the euclidean distance. Then we calculate the synthesized empirical mean for the target domain embeddings according to Eq. 3,

$$\hat{\mu}^t, \hat{\sigma}^t = \frac{\hat{\mathbf{f}}^t + \sum_{k \in I_c^t} \mu_k^t}{K+1}, \frac{\sum_{k \in I_c^t} \sigma_k^t}{K} + \alpha, \quad (3)$$

where α is a fixed factor. Then we build up a multi-variant normal distribution based on the synthesized empirical mean and covariance according to Eq. 4.

$$\hat{\mathbf{f}}_{\text{new}}^t = \frac{1}{\hat{\sigma}^t \sqrt{2\pi}} e^{-\frac{(\hat{\mathbf{f}}^t - \hat{\mu}^t)^2}{2(\hat{\sigma}^t)^2}}. \quad (4)$$

Additional embeddings can be derived by leveraging the established normal distributions for each temporal snippet within the target domain. The new generated features $\hat{\mathbf{f}}_{\text{new}}^t$ share the same class with $\hat{\mathbf{f}}^t$. This process utilizes statistical parameters obtained from the source domain, in conjunction with the provided few-shot samples from the target domain. The purpose of this approach is to enhance diversity within the latent space while simultaneously reasoning information from both the source and target domains.

Temporal Relational Attention Network with Relation Dropout (TRAN-RD). When considering adapting the model into another domain by a few samples, a temporal aggregation approach with great generalizability will help to grasp the important cues from different temporal relations. To delve into this concern, we propose a new temporal aggregation mechanism, *i.e.*, temporal relational attention network with relation dropout, which incorporates two major concepts, *i.e.*, Relation-Dropout based Multi-Head Self-Attention (RD-MHSA) and Scale-wise Multi-Head Self-Attention (Scale wise-MHSA), to attend on different temporal relational granularities, and learn representative and generalizable features. We first generate multi-scale relational index sets as Eq. 5,

$$\Omega_r = \{(i, \dots, k, \dots, j) | i \leq \dots \leq k \leq \dots \leq j, \\ (i, \dots, k, \dots, j) \in [1, N_T]^r, \text{ and } r \in [2, N_T]\}, \quad (5)$$

where we can grasp relational indexes according to different scales. The selected snippets preserve the temporal order. r is used to define the selected scales of the desired relational set. Relation-Dropout Multi-Head Self-Attention (RD-MHSA) is used first to aggregate the temporal features within each snippet. The relational attended snippet embedding $\hat{\mathbf{f}}_s$ for one snippet \mathbf{f}_s from the given snippet relation set $\Omega_s \in \Omega_r$ can be calculated through Eq. 6,

$$\mathbf{f}_a = LN(SM(\frac{\mathbf{P}_Q(\mathbf{f}_s) \cdot \mathbf{P}_K(\mathbf{f}_s)}{\sqrt{d_k}}) * \mathbf{P}_V(\mathbf{f}_s)), \quad (6)$$

$$\hat{\mathbf{f}}_s = LN(\mathbf{f}_s + \sum_{h=1}^{N_h} \mathbf{f}_a^h + FFN(\mathbf{f}_s)), \quad (7)$$

where LN indicates layer normalization, SM indicates the SoftMax operation, and FFN indicates a multi-layer-perception (MLP) based Feed-Forward Network. d_k is a scale factor. \mathbf{P}_Q , \mathbf{P}_K , and \mathbf{P}_V are chosen as linear projections. \mathbf{f}_a^h indicates the relational attention obtained through N_h heads. After the aforementioned process, we obtain the self-attended relation set $\hat{\Omega}_s$. Then, we apply dropout to the snippets within each attended relation set as Eq. 8.

$$\hat{\Omega}_s^{DP} = DropOut(\hat{\Omega}_s, \beta), \quad (8)$$

where β is the pre-defined dropout ratio for the snippets inside one relation set. The RD-MSHA aims at learning representative features when snippets are randomly not available in the training procedure.

Scale-wise Multi-Head Self-Attention (Scale-wise MHSA) is then used to aggregate the information within each scale. We first do concatenation considering all snippets inside one relation set after the relation dropout along the temporal dimension, denoted as $\hat{\mathbf{f}}_s^{\Omega_s}$. Then we regard the temporal dimension as the token dimension for MHSA. Scale-wise MHSA is then achieved by Eq. 9 and Eq. 10,

$$\hat{\mathbf{f}}_a^{\Omega_s} = LN(SM(\frac{\hat{\mathbf{P}}_Q(\hat{\mathbf{f}}_s^{\Omega_s}) \cdot \hat{\mathbf{P}}_K(\hat{\mathbf{f}}_s^{\Omega_s})}{\sqrt{\hat{d}_k}}) * \hat{\mathbf{P}}_V(\hat{\mathbf{f}}_s^{\Omega_s})), \quad (9)$$

$$\tilde{\mathbf{f}}_a^{\Omega_s} = LN(\hat{\mathbf{f}}_s^{\Omega_s} + \sum_{h=1}^{N_h} \hat{\mathbf{f}}_a^{\Omega_s, h} + FFN(\hat{\mathbf{f}}_s^{\Omega_s})), \quad (10)$$

where all the projections $\hat{\mathbf{P}}_Q$, $\hat{\mathbf{P}}_K$, and $\hat{\mathbf{P}}_V$ are chosen as linear projections. \hat{d}_k is fixed scale factor. Then we calculate the final aggregated feature through Eq. 11.

$$\mathbf{f}^* = \frac{\sum_{\Omega_s \in \Omega_r} \tilde{\mathbf{f}}_a^{\Omega_s}}{N_s}, \quad (11)$$

where N_s denotes the total number of the scales.

Cross Domain Information Alignment (CDIA). After the enrichment of the latent space features and the development of a generalizable temporal relation aggregation method, we further try to introduce more constraints during learning to bridge the gap between the source domain and target domain by using the provided few-shot target domain samples. When a source domain anchor is given as \mathbf{f}_a^* after the TRAN-RD, we wish it could be closer to its corresponding cluster centers \mathbf{f}_c^* calculated on the target domain while being far away from the negative anchors $\tilde{\mathbf{f}}_n^*$ from different categories. The CDIA loss can be therefore calculated via Eq. 12,

$$\mathcal{L}_{CDIA} = -\frac{1}{N} \sum_{i=1}^N \log \frac{e^{(\cos(\mathbf{f}_{(i,a)}^*, \mathbf{f}_{(i,c)}^*))}}{\sum_{j=1}^{N_n} e^{(\cos(\mathbf{f}_{(i,a)}^*, \tilde{\mathbf{f}}_{(i,j)}^*))}}, \quad (12)$$

where N denotes the sample number from the source domain and N_n denotes the number of the negative anchors for the i -th anchor. \cos indicates the cosine similarity. $\mathbf{f}_{(i,c)}^*$ indicates the target domain center for i -th anchor within class c . The target domain few-shot cluster centers can be calculated through Eq. 13.

$$\mathbf{f}_c^* = \frac{\sum_{i=1}^{N_c} \mathbf{f}_{(i,c)}^*}{N_c}, \quad (13)$$

where N_c indicates the sample number for the class c and \mathbf{f}_c^* indicates the target domain center for class c . Apart from the CDIA loss, we make use of supervised cross-entropy losses for both the samples from the source domain training set, target domain few-shot training set, and target domain generated training set, *i.e.*, L_{CES} , L_{CET} , and L_{CEA} . In order to get representative features from the generated target domain training set, we make use of another contrastive learning loss through Eq. 14,

$$\mathcal{L}_{aux} = -\frac{1}{N_g} \sum_{i=1}^{N_g} \log \frac{e^{(\cos(\mathbf{f}_{(i,a)}^+, \mathbf{f}_{(i,p)}^+))}}{\sum_{j=1}^{N_n} e^{(\cos(\mathbf{f}_{(i,a)}^+, \mathbf{f}_{(j,n)}^+))}}, \quad (14)$$

where the positive anchors \mathbf{f}_p^+ are generated through random permutation of the input snippet along the temporal axis while the negative anchor \mathbf{f}_n^+ is the sample from different classes. N_g indicates the number of the generated features in the shared latent space. \cos denotes cosine similarity. The supervision is thereby achieved through a weighted sum of the aforementioned loss functions by Eq. 15.

$$L_{all} = \omega_1 * L_{CDIA} + \omega_2 * L_{CES} + \omega_3 * L_{CET} + \omega_4 * L_{CEA} + \omega_5 * \mathcal{L}_{aux}. \quad (15)$$

TABLE I: Experimental results on UCF [20] \rightarrow HMDB [19], HMDB [19] \rightarrow UCF [20], and EPIC-KITCHEN [1].

Method		① UCF → HMDB				② HMDB → UCF				③ EPIC-KITCHEN mean				④ Sims4Action → ToyotaSmartHome			
		S-1	S-5	S-10	S-20	S-1	S-5	S-10	S-20	S-1	S-5	S-10	S-20	S-1	S-5	S-10	S-20
DG	Random			8.6				8.1				12.5				11.1	
	KNN			81.1				88.3				28.1				3.3	
	Nearest Center			83.9				91.5				27.4				28.0	
	Nearest Neighbor			80.1				88.6				25.5				3.27	
FSDA-AR	CoMix [5]	83.1	88.1	89.7	90.8	91.0	93.2	96.8	96.3	31.2	31.8	32.1	32.7	24.2	20.6	28.9	35.5
	CO ² A [27]	83.9	88.1	89.1	91.1	92.5	94.0	96.7	97.5	32.6	36.4	38.0	38.2	21.9	26.6	34.0	42.1
	TA ³ N [3]	83.3	88.9	88.3	91.7	93.7	95.1	97.5	98.0	37.9	41.2	42.1	43.0	21.1	29.8	35.8	42.7
	TranSVAE [4]	82.3	82.8	83.2	84.8	89.7	89.0	94.4	95.1	37.6	41.1	40.8	43.3	22.6	22.7	18.9	22.7
	TRX [48]	77.2	80.3	78.6	81.9	82.2	83.1	81.1	84.4	26.7	27.4	28.7	30.2	14.0	13.8	19.0	18.9
	HyRSM [49]	79.7	81.1	82.2	83.6	88.1	90.1	91.0	90.8	35.8	36.7	37.1	37.8	18.9	22.4	27.4	28.0
	FS-ADA [16]	82.7	87.2	88.6	87.2	91.9	94.4	93.7	96.5	37.0	39.7	39.3	40.4	17.1	22.6	28.3	28.0
	PASTN [15]	83.4	86.2	88.3	89.8	91.2	94.2	95.8	96.5	36.1	40.5	40.3	42.5	22.6	22.6	22.6	28.0
	SSA ² lign [17]	80.6	85.0	88.3	87.8	87.0	94.4	94.6	94.4	31.5	40.1	40.9	42.0	22.6	23.7	35.0	41.3
RelaMiX (ours)		85.6	91.1	91.1	92.2	94.1	97.2	97.9	98.4	40.7	43.9	44.4	45.2	27.0	31.0	38.9	49.2

IV. EXPERIMENTAL RESULTS

A. Datasets

We utilize five popular human activity recognition datasets, *e.g.*, HMDB-51 [19], UCF-101 [20], EPIC-KITCHENS-55 [1], ToyotaSmartHome (TSH) [18], and Sims4Action [2], to investigate FSDA-AR. The selected datasets comprise diverse activities and recording environments, enabling comprehensive evaluation of DA techniques. The group of the methods that are under *DG* only use the samples from the source domain, while the methods that are under *FSDA-AR* make use of the samples from both the source and target domain.

HMDB-51 [19] contains 6,766 video clips from various sources, spanning across 51 activities categories with a minimum of 101 clips per activity. 12 action classes are chosen to formulate the domain adaptation task.

UCF-101 [20] consists of 13,320 video clips, divided into 101 activity categories. These datasets are employed in the HMDB \rightarrow UCF and UCF \rightarrow HMDB adaptation tasks where they share 12 classes.

EPIC-KITCHENS-55 [1] comprises 55 hours of egocentric videos, capturing kitchen activities performed by 32 participants, and is utilized in the Epic-Kitchens domain adaptation task. We make use of the domain adaptation benchmark defined by [51] on 8 overlapped activities.

ToyotSmartHome (TSH) [18] includes 16,115 video clips, containing 31 daily living activities, 10 of which are chosen to formulate the domain adaptation in our benchmark.

Sims4Action [2] is a synthetic dataset specifically designed for cross-domain evaluation on TSH. It comprises 13,232 video clips, depicting 10 daily living activities performed by avatars in the Sims 4 game, these datasets are used in the Sims4Action \rightarrow TSH adaptation task. These datasets serve as a robust foundation for exploring DA techniques in various cross-domain scenarios, offering challenges inherent in real-world and synthetic video data.

B. Implementation Details

We randomly select N_{shot} samples per class on the target domain training set to construct our benchmarks, where $N_{shot} \in \{1, 5, 10, 20\}$ (1~20). The few-shot samples

are fixed to achieve better knowledge guidance through co-training by using the information provided by the source and target domains. To make a fair comparison, all the feature extraction backbone is unified as I3D [34] initialized with Kinetics400 [50] pre-trained weight. Our model is trained on an NVIDIA-A100 GPU using PyTorch 1.12 with a batch size of 32, step-wise learning rate decaying at epoch 60 and 80, and the Adam optimizer [52] with an initial learning rate of 0.0001 for 100 epochs. The sliding window size for the feature extraction is set as $N_w = 16$ while temporal zero padding 8 is used. $K = 2$ is chosen for the SDFM. Considering the weights of the losses, $\omega_1 = 0.0001$, $\omega_2 = 1$, $\omega_3 = 1$, $\omega_4 = 0.01$, and $\omega_5 = 0.0001$, respectively. β in the TRAN-RD is chosen as 0.5. The head's number of RD-MHSA and Scale-wise MHSA is chosen as 8. In SDFM, α is chosen as 0.21, and 200 samples are generated for each activity category.

C. Analysis of the Benchmark

The performance results for the transfer tasks involving the UCF [20] to HMDB [19], HMDB to UCF, EPIC-KITCHEN [1], and Sims4Action [2] to ToyotaSmartHome (TSH) settings are presented in Table I (①, ②, ③, and ④), respectively. We also provide per-split performances on the EPIC-KITCHEN in Table II. Both UDA methods, implemented within the context of the FSDA-AR task, as well as previously published FSDA-AR techniques, show notable performance, consistently outperforming random baseline benchmarks. This observation underscores the effective reduction of domain gaps when utilizing a limited number of labeled shots. Notably, the reduction in the required number of target domain samples is substantial when we compare FSDA-AR with the well-established UDA task. For instance, in a scenario with only 5 labeled shots, the total required sample count is approximately only 1.6% of that used in conventional UDA setting on EPIC-KITCHEN D1 \rightarrow D2. However, it is noteworthy that the TranSVAE method [4] exhibits inferior performance in the FSDA-AR task, even though it outperforms TA³N [3] in the context of UDA task, as reported in Table III.

This discrepancy suggests that the disentanglement method applied in the context of domain adaptation relies heavily on the availability of large-scale data from the target domain to effectively capture adaptation cues. Similar trends can be

TABLE II: Experimental results on the EPIC-KITCHEN [1] dataset considering six different adaptation settings.

Method		① D1 → D2				② D2 → D1				③ D1 → D3				④ D3 → D1				⑤ D2 → D3				⑥ D3 → D2			
		S-1	S-5	S-10	S-20	S-1	S-5	S-10	S-20	S-1	S-5	S-10	S-20	S-1	S-5	S-10	S-20	S-1	S-5	S-10	S-20	S-1	S-5	S-10	S-20
DG	Random		12.5					12.3				12.7			12.6				12.3					12.4	
	KNN		25.5					26.9				26.2			27.4				28.5					33.9	
	Nearest Center		24.0					29.2				29.2			25.1				34.0					23.1	
	Nearest Neighbor		22.1					24.9				26.6			26.4				24.1					28.7	
FSDA-AR	CoMix [5]	31.5	32.0	34.3	35.7	25.2	27.9	31.1	29.9	30.0	30.4	28.5	30.8	30.4	30.2	28.8	30.4	34.0	34.5	35.3	34.4	36.0	35.7	34.5	35.1
	CO ² A [27]	31.7	33.5	33.6	33.3	32.6	38.4	36.1	39.8	30.2	36.4	38.3	38.0	34.0	36.6	40.5	40.0	34.7	36.6	40.5	40.0	32.6	36.8	39.0	38.6
	TA ³ N [3]	36.8	39.0	40.2	43.5	36.8	38.9	40.4	40.5	36.7	40.2	41.0	40.3	33.1	40.0	40.9	41.8	41.1	43.4	43.5	45.6	42.8	45.8	46.5	46.5
	TransVAE [4]	32.9	39.5	39.5	42.8	35.3	40.4	37.5	41.7	37.0	39.1	40.3	42.3	36.1	38.2	37.5	41.4	42.8	44.9	44.5	45.9	41.2	44.4	45.6	45.6
	TRX [48]	24.8	25.0	25.2	25.9	26.1	27.7	30.7	31.6	25.3	25.9	28.1	28.8	26.6	28.9	29.3	30.0	28.4	28.0	30.6	31.9	28.8	29.1	28.4	33.1
	HyRSM [49]	31.1	33.5	34.0	37.2	33.4	32.7	33.9	34.8	33.2	37.2	36.5	36.7	35.0	34.8	35.7	35.0	40.4	40.3	41.2	41.4	41.6	41.8	41.5	41.5
	FS-ADA [16]	36.4	38.1	38.4	37.7	34.7	36.8	39.1	39.3	36.1	37.4	38.2	40.5	32.2	39.8	35.9	38.6	42.4	42.5	42.0	44.3	40.4	43.5	42.1	42.2
	PASTN [15]	33.3	38.2	37.7	41.3	34.0	38.9	36.8	40.9	35.3	39.4	39.0	41.0	33.6	37.9	38.2	41.1	39.2	43.1	44.4	44.6	43.0	45.5	45.9	45.8
	SSA ² lign [17]	32.0	40.4	37.6	41.5	31.3	40.1	40.5	41.6	30.1	39.3	42.0	42.6	34.5	38.9	41.1	39.1	28.7	42.9	42.1	44.5	32.3	38.7	41.9	42.7
	RelaMiX (ours)	39.1	43.9	43.7	47.9	38.4	41.6	42.1	42.8	38.4	42.1	42.5	43.1	37.9	41.6	42.3	42.5	45.1	46.2	47.4	46.5	45.5	48.0	48.1	48.1



Fig. 3: Qualitative results for FSDA-AR on 20-Shot Sims4Action [2] → TSH [18].

observed in the case of the CoMix approach [5], which relies on the diversity of backgrounds in the target domain to achieve adaptation, particularly in scenarios involving datasets with substantial domain gaps. In all our experiments, we employ the I3D backbone [34] to ensure equitable comparisons. To facilitate an assessment relative to the SSA²Lign approach [17], we replace the TimesFormer [33] backbone in SSA²Lign with the I3D [34] backbone. The reduction in performance observed in the adapted SSA²Lign model when applied to the leveraged datasets can be attributed to two primary factors.

Firstly, it stems from disparities in domain gaps in our experimental configurations. Secondly, it arises from SSA²Lign's reliance on transformer features sourced from the TimesFormer [33] backbone. However, to ensure an equitable comparison with methods tailored for UDA tasks, it is imperative to standardize the backbone as I3D [34]. The rationale behind this standardization is that I3D is commonly employed in UDA works, thereby allowing us to effectively demonstrate that the observed performance enhancements are a consequence of

our proposed method, rather than a consequence of backbone substitution. To maximize the utility of the limited target-domain samples provided, we take into account three crucial elements concerning the latent space source domain feature generation, the generalizability of the temporal aggregator considering multi-scale relationships, and the inter-domain alignment by using target-domain prototypes.

Comparing against the best baseline for each shot-setting, our proposed RelaMiX achieves 2.8%, 2.7%, 2.3%, and 1.9% performance improvement for 1~20-shot setting on EPIC-KITCHEN [1] in terms of FSDA-AR in Table I ③. The per-split performances are showcased in Table II, where RelaMiX shows consistent superior results on the FSDA-AR task for each split of EPIC-KITCHEN [1]. Some UDA approaches implemented into FSDA-AR do not show better performances compared with statistic baselines, indicating that fewer target domain samples may cause overfitting to some approaches that require a large number of samples, especially on the datasets with large domain differences, *e.g.*, CoMix [5] on

TABLE III: Task comparison between FSDA-AR and UDA.

Method	Shot-1	Shot-5	Shot-10	Shot-20
① UDA approaches on UDA task on EPIC-KITCHEN.				
TranSVAE [4]		52.6		
CoMix [5]		43.2		
TA ³ N [3]		39.9		
DANN [6]		39.2		
ADDA [53]		39.2		
② TA³N and RelaMiX on FSDA-AR task on EPIC-KITCHEN.				
TA ³ N [3]	38.9	41.8	42.1	43.0
RelaMiX (ours)	41.0	44.4	44.5	45.1
③ UDA approaches for UDA tasks on UCF → HMDB.				
TranSVAE [4]		87.8		
CoMix [5]		86.7		
TA ³ N [3]		81.4		
DANN [6]		80.1		
ADDA [53]		79.2		
④ TA³N and RelaMiX for FSDA-AR task on UCF → HMDB.				
TA ³ N [3]	83.3	88.9	88.3	91.7
RelaMiX (ours)	84.4	89.7	90.3	92.8
⑤ UDA approaches for UDA tasks on HMDB → UCF.				
TranSVAE [4]		99.0		
CoMix [5]		93.9		
TA ³ N [3]		90.5		
DANN [6]		88.1		
ADDA [53]		88.4		
⑥ TA³N and RelaMiX for FSDA-AR task on HMDB → UCF.				
TA ³ N [3]	93.7	95.1	97.5	98.0
RelaMiX (ours)	95.6	96.5	97.7	98.2
⑦ UDA approaches for UDA task on Sims4Action → TSH.				
Schneider <i>et al.</i> [54]		36.3		
TA ³ N [3] ([54])		8.0		
⑧ TA³N and RelaMiX for FSDA-AR task on Sims4Action → TSH.				
TA ³ N [3]	21.1	29.8	35.8	42.7
RelaMiX (ours)	24.6	31.4	36.7	45.7

EPIC-KITCHEN [1].

Regarding the FSDA-AR task on the UCF [20] → HMDB [19] and HMDB [19] → UCF [20] introduced in Table I ① and ②, all the approaches show promising performance even under 1-shot. When $N_{shot} \geq 5$ on the UCF [20] → HMDB [19], CoMix [5], CO²A [27], and TA³N [3] under FSDA-AR are better than the state-of-the-art performance 87.8% delivered by TranSVAE for UDA task as in Table III ①, which demonstrates that FSDA-AR is more efficient compared with UDA when facing with small domain gap. Compared with the approach with the best performance among all the baselines for 1~20 shot settings, RelaMiX achieves performance improvements with 1.7%, 2.2%, 1.4%, and 0.5% for FSDA-AR on the UCF [20] → HMDB [19] and 0.4%, 2.1%, 0.4%, and 0.4% on the HMDB [19] → UCF [20], respectively. Compared with the baseline with the best performance for 1-20 shot settings on Sims4Action [2] → TSH [18], RelaMiX achieves performance improvements with 2.8%, 1.2%, 3.1%, and 6.5%, introduced in Table II ④. The consistent performance enhancements produced by RelaMiX across various datasets indicate that the proposed method effectively utilizes the guidance provided by the few-shot labeled samples from the target domain. Furthermore, RelaMiX can achieve a generalizable temporal aggregation that accounts for diverse domain differences. In

TABLE IV: Module ablation for RelaMiX on EPIC-KITCHEN [1] D1 → D2 considering different shots from the target domain.

Method	S-1	S-5	S-10	S-20
w/o TARD-RD	36.3	40.3	40.9	44.1
w/o CDIA	37.9	41.3	40.7	47.2
w/o SDFM	34.7	42.5	42.3	45.3
w/ All	39.1	43.9	43.7	47.9

TABLE V: Module ablation for TRAN-RD mechanism on EPIC-KITCHEN [1] D1 → D2 considering different shots from the target domain.

Method	S-1	S-5	S-10	S-20
w/o RD-MHSA	31.6	37.1	39.2	39.2
w/o Scale-wise MHSA	28.1	37.9	39.3	39.3
w/o RD	32.3	39.5	37.3	39.7
w/ All	39.1	43.9	43.7	47.9

terms of video-based domain adaptation, the FSDA-AR task exhibits comparable performance to the UDA task for human activity recognition, as reported in Table III. Consequently, our experiments confirm the feasibility of FSDA-AR and we believe it to be an essential future research direction in domain adaptation for human activity recognition.

D. Ablation Studies

Ablation of the Individual Concept. To assess the efficacy of each proposed mechanism, we conduct ablation experiments on the EPIC-KITCHEN [1] dataset, specifically the D1 → D2 split, as detailed in Table IV. Initially, we compare RelaMiX against RelaMiX w/o TARD-RD, employing Temporal Relation Networks (TRN) as an alternative for temporal aggregation. The results indicate that RelaMiX outperforms RelaMiX w/o TARD-RD, achieving performance improvements of 2.8%, 3.6%, 2.8%, and 3.8% across 1~20 shot settings. These findings highlight the superiority of our TRAN-RD method for temporal aggregation in the FSDA-AR task. The integration of relational attention with relation dropout and scale-wise self-attention is verified effective in facilitating generalizable temporal aggregation and feature learning.

Subsequently, we compare RelaMiX with RelaMiX w/o the SDFM component. In this scenario, RelaMiX demonstrates superiority over its SDFM-lacking counterpart, exhibiting performance improvements of 4.4%, 1.4%, 1.4%, and 2.6% for the 1~20 shot settings. These results indicate that SDFM effectively enhances the latent space embeddings of the target domain. Finally, a comparison is made between RelaMiX and RelaMiX w/o CDIA. RelaMiX outperforms the CDIA-lacking variant by 1.2%, 2.6%, 3.0%, and 0.7% for the 1~20 shot settings, revealing that CDIA plays a significant role in bridging the domain gap by extracting pertinent information from a limited number of target-domain samples. Notably, the contributions of each component in the proposed solution vary across the different shot settings.

Ablation of the TRAN-RD. We deliver the ablation experiments of the TRAN-RD in Table V, where *w/o RD*-

TABLE VI: Module ablation for CDIA on EPIC-KITCHEN [1] D1 \rightarrow D2 considering different shots from the target domain.

Method	S-1	S-5	S-10	S-20
w/o prototypes	31.5	35.7	35.7	42.5
w/o mixed domain negatives	34.4	38.3	37.2	39.3
w/ All	39.1	43.9	43.7	47.9

TABLE VII: Module ablation for SDFM on EPIC-KITCHEN [1] D1 \rightarrow D2 considering different shots from the target domain.

Method	S-1	S-5	S-10	S-20
K=1	33.6	38.4	39.1	44.5
K=3	32.7	38.0	38.5	43.6
K=4	34.9	39.3	38.8	43.9
K=2	39.1	43.9	43.7	47.9

MHSA means that the RD-MHSA is replaced by multi-layer perceptron (MLP), *w/o Scale-wise MHSA* means that we use mean average to achieve multi-scale aggregation, and *w/o RD* indicates that the relation dropout is discarded. First, when we compare TRAN-RD with the variant *w/o RD-MHSA*, we find out that by using RD-MHSA, the model can achieve 7.5%, 6.8%, 4.5%, and 8.7% performance improvements for FSDA-AR considering 1~20 shot settings, which showcases the importance of the RD-MHSA on snippet-wise temporal information aggregation in our RelaMiX. Then, we compare TRAN-RD with the ablation *w/o Scale-wise MHSA*, we observe that Scale-wise MHSA can achieve performance gains of 11.0%, 6.0%, 4.4%, and 8.6% for 1~20 shot settings, indicating the superiority of the scale-wise information reasoning ability of this superior design. Finally, to showcase the importance of the relation dropout design, we compare TRAN-RD with *w/o RD*, where the relation dropout brings a performance boost by 6.8%, 4.4%, 6.4%, and 8.2% for the 1~20 shot settings, respectively. This ablation study demonstrates the collaboration of each part of the module design helps to obtain a generalizable temporal aggregator for the FSDA-AR setting.

Ablation of the CDIA. We conduct ablation experiments in Table VI to demonstrate the reason behind the supervision design. Two ablation experiments are executed for CDIA, which are *w/o prototypes* by replacing the prototype-based positive anchors with the randomly temporal permuted anchor embedding, and *w/o mixed domain negatives* by replacing the mixed domain negatives with the source-domain negative anchor embeddings. Compared with variant *w/o prototypes*, using the target domain prototypes as the positive anchors achieves performance improvements of 7.6%, 8.2%, 8.0%, and 5.4% for the 1~20 shot settings.

Compared with *w/o mixed domain negatives*, using the domain negatives achieves performance improvements of 4.7%, 5.6%, 6.5%, and 8.6% for the 1~20 shot settings. The aforementioned observations turn out that mixed domain negatives and target domain prototypes collaborate together to contribute a more reasonable FSDA-AR supervision when only few-shot

TABLE VIII: Comparison between TRAN-RD with other temporal aggregation methods on EPIC-KITCHEN [1] D1 \rightarrow D2 considering different shots from the target domain. The GFLOPS are provided, while all the methods share the same feature extractor I3D [34] with 108 GFLOPS.

Method	GFLOPS	S-1	S-5	S-10	S-20
LSTM	0.09	31.3	40.9	35.2	37.7
GRU	0.10	32.5	32.9	36.5	39.1
TRN	0.04	33.2	43.1	40.1	41.5
TRAN-RD	0.92	39.1	43.9	43.7	47.9

target domain samples are available.

Ablation of the SDFM. We conduct the ablation study for SDFM in Table VII to observe the influence brought by different numbers of cluster centers, where the experiments are done for $K \in \{1, 2, 3, 4\}$. We found the setting $K = 2$ generally works well for the feature mixture.

Comparison with Other Temporal Aggregators. We further conduct a comparison study among TRAN-RD and other existing temporal aggregators, *i.e.*, LSTM, GRU, and TRN [55], in Table VIII. Our TRAN-RD outperforms all the others by a large margin for the 1~20 shot settings. TRN can achieve a good performance on the 5~20 shot settings, however, it can not achieve a generalizable temporal aggregation by using an extremely small shot number, *e.g.*, on 1 shot setting, which is an important setting when the data in the target domain is extremely hard to acquire. The other temporal aggregators, *e.g.*, LSTM and GRU, also have the aforementioned problem.

Our proposed TRAN-RD overcomes this difficulty by using superior relation-based techniques to achieve temporal aggregation in different scale settings. Alongside the recognition performances, we also provide GFLOPS of different temporal aggregators to illustrate the computational difficulties of our approach during inference. Since all the baselines chosen in our benchmark are unified to use I3D [34] as the feature extractor, which takes the most of the computational complexity, *i.e.*, 108 GFLOPS, directly comparing the GFLOPS of the temporal aggregator will be more obvious. Our TRAN-RD brings a computational complexity increase by 0.92 GFLOPS due to the leverage of the RD-MHSA and Scale-wise MHSA mechanism. However, this increase is small compared with the GFLOPS of the video backbone I3D [34] with 108 GFLOPS. Moreover, CDIA and SDFM only participate in the training phase and they do not contribute to the computational complexity during the inference time.

E. Analysis of Qualitative Results

Apart from the quantitative analysis, we further assess qualitative results from the proposed FSDA-AR task. As shown in ①–⑩ in Figure 3, we visualize ten results of activity recognition from the setting of 20-shot Sims4Action \rightarrow TSH, including all of the ten classes leveraged for FSDA-AR. For each sample, we compare the activity predictions from FS-ADA [16], TA³N [3], SSA²Lign [17], PASTN [15], and our RelaMiX, respectively. Since the domain gap between the

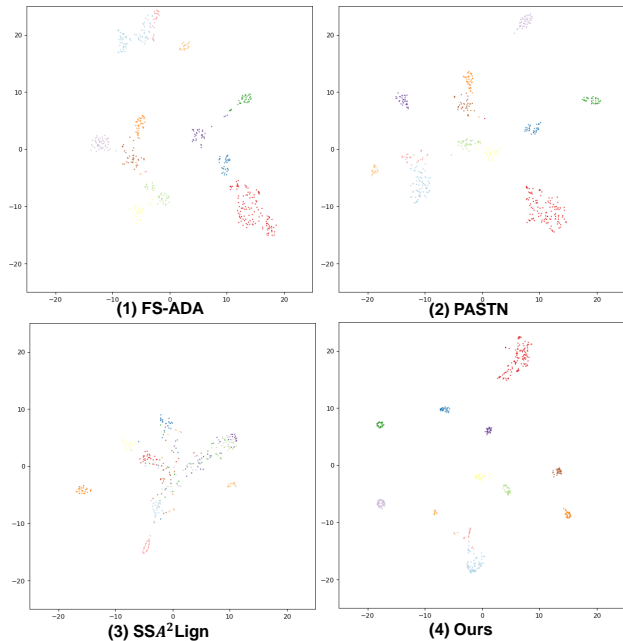


Fig. 4: The t-SNE feature visualization [56] on the UCF test set [20] for FSDA-AR on 20-Shot HMDB [19] → UCF [20].

synthesized dataset and the real dataset is large, most of the leveraged baselines can not guarantee superior performances.

Thanks to the proposed method which takes the temporal generalizability, the diversity of the latent space, and the cross-domain alignment into consideration, our RelaMiX obtains much better generalization ability and yields state-of-the-art results when performing the few-shot domain adaptation for video data. Our RelaMiX approach correctly classifies eight out of ten samples considering such a challenging setting. The qualitative results are consistent with the assumption that the model can benefit from the proposed techniques and obtain generalizable temporal aggregation as well.

F. Analysis of the t-SNE Visualization

To investigate the performance of few-shot domain adaptation on latent space, t-SNE distribution [56] is presented in Figure 4. From (a) to (d) are the t-SNE distributions from FS-ADA, PASTN, TA³N, and our RelaMiX. Under the setting of HMDB [19] → UCF [20], the samples shown in Figure 4 are selected from the UCF101 test set. Compared to the other methods, the features from our RelaMiX are more distinguishable across different classes in the latent space, showing a better generalization ability of RelaMiX, which is crucial in FSDA-AR.

G. Analysis of the Target Domain Sample Number of FSDA-AR and UDA

We present the required sample number to formulate the training set on the target domain separately for FSDA-AR and UDA tasks on all the leveraged DA settings in Table IX. Compared with UDA, FSDA-AR requires obviously less data on the target domain for training. Since the labeling work

TABLE IX: Analysis of the sample number that is required for FSDA-AR and UDA under each setting.

Setting	FSDA				UDA
	S-1	S-5	S-10	S-20	
UCF [20]→HMDB [19]	12	60	120	240	840
HMDB [19]→UCF [20]	12	60	120	240	1438
Sims4Action [2]→TSH [18]	10	50	100	200	8552
D1→D2 [1]	8	40	80	160	2495
D2→D1 [1]	8	40	80	160	1543
D2→D3 [1]	8	40	80	160	3897
D3→D2 [1]	8	40	80	160	2495
D1→D3 [1]	8	40	80	160	3897
D3→D1 [1]	8	40	80	160	1543

for activity recognition is not pixel-wise annotation and each sample only needs one label, the data collection may need more time than labeling one sample. In that case, our training set on the target domain for the 20-shot setting needs obviously less time compared with the UDA task on each DA setting. On Sims4Action → TSH, 97.7% of the samples from the target domain for the training are discarded in FSDA-AR compared with UDA, while FSDA-AR delivers a better performance. The performance of FSDA-AR is comparable to UDA as mentioned before, which indicates that FSDA-AR is a more efficient setting, especially when the data collection in the target domain is hard to execute.

We point out that FSDA-AR is an important research direction in the future and our work will serve as an important test bed in this direction.

V. CONCLUSION

In this study, we have explored the research domain of video-based human activity recognition within the context of Few-Shot Domain Adaptation (FSDA-AR). Our contributions include the establishment of a comprehensive FSDA-AR benchmark encompassing five datasets, which incorporate diverse real-world, egocentric, and synthetic video data. We have introduced RelaMiX, a novel solution characterized by a Temporal Relational Attention Network with Relation Dropout (TRAN-RD), a Statistic Distribution-Based Feature Mixture (SDFM) method, and a Cross-Domain Information Alignment (CDIA) supervision approach. Our findings showcase that the proposed RelaMiX attains state-of-the-art performances across various FSDA-AR scenarios in human activity recognition, demonstrating its robustness on multiple benchmarks and within diverse few-shot settings.

Importantly, our observations highlight that RelaMiX can achieve domain adaptation performance that is on par with Unsupervised Domain Adaptation (UDA) methods while using noticeably fewer samples from the target domain. This underscores the significance of FSDA-AR as a promising research avenue for enhancing data efficiency in domain adaptation tasks. It represents a promising future direction for the field, emphasizing the potential for reduced data requirements while maintaining high adaptation performance.

REFERENCES

- [1] D. Damen *et al.*, “Scaling egocentric vision: The EPIC-KITCHENS dataset,” in *Proc. ECCV*, vol. 11208, Sep. 2018, pp. 753–771.

- [2] A. Roitberg, D. Schneider, A. Djamal, C. Seibold, S. Reiß, and R. Stiefelhagen, "Let's play for action: Recognizing activities of daily living by learning from life simulation video games," in *Proc. IORS*, Sep. 2021, pp. 8563–8569.
- [3] M. Chen, Z. Kira, G. Alregib, J. Yoo, R. Chen, and J. Zheng, "Temporal attentive alignment for large-scale video domain adaptation," in *Proc. ICCV*, Oct. 2019, pp. 6320–6329.
- [4] P. Wei *et al.*, "Unsupervised video domain adaptation for action recognition: A disentanglement perspective," in *Proc. NeurIPS*, Dec. 2023.
- [5] A. Sahoo, R. Shah, R. Panda, K. Saenko, and A. Das, "Contrast and mix: Temporal contrastive video domain adaptation with background mixing," in *Proc. NeurIPS*, vol. 34, Dec. 2021, pp. 23 386–23 400.
- [6] Y. Ganin and V. S. Lempitsky, "Unsupervised domain adaptation by backpropagation," in *Proc. ICML*, vol. 37, Jul. 2015, pp. 1180–1189.
- [7] G. Kang, L. Jiang, Y. Yang, and A. G. Hauptmann, "Contrastive adaptation network for unsupervised domain adaptation," in *Proc. CVPR*, Jun. 2019, pp. 4893–4902.
- [8] J. Choi, G. Sharma, S. Schuler, and J. Huang, "Shuffle and attend: Video domain adaptation," in *Proc. ECCV*, vol. 12357, Aug. 2020, pp. 678–695.
- [9] Y. Xu, J. Yang, H. Cao, K. Wu, M. Wu, and Z. Chen, "Source-free video domain adaptation by learning temporal consistency for action recognition," in *Proc. ECCV*, vol. 13694, Oct. 2022, pp. 147–164.
- [10] K. Saito, D. Kim, S. Sclaroff, T. Darrell, and K. Saenko, "Semi-supervised domain adaptation via minimax entropy," in *Proc. ICCV*, Oct. 2019, pp. 8049–8057.
- [11] L. Yang *et al.*, "Deep co-training with task decomposition for semi-supervised domain adaptation," in *Proc. ICCV*, Oct. 2021, pp. 8886–8896.
- [12] J. Yoon, D. Kang, and M. Cho, "Semi-supervised domain adaptation via sample-to-sample self-distillation," in *Proc. WACV*, Jan. 2022, pp. 1686–1695.
- [13] J. Li, G. Li, Y. Shi, and Y. Yu, "Cross-domain adaptive clustering for semi-supervised domain adaptation," in *Proc. CVPR*, Jun. 2021, pp. 2505–2514.
- [14] J. Fan, Z. Zhang, T. Tan, C. Song, and J. Xiao, "CIAN: Cross-image affinity net for weakly supervised semantic segmentation," in *Proc. AAAI*, vol. 34, no. 07, Feb. 2020, pp. 10 762–10 769.
- [15] Z. Gao, L. Guo, W. Guan, A. Liu, T. Ren, and S. Chen, "A pairwise attentive adversarial spatiotemporal network for cross-domain few-shot action recognition-R2," *TIP*, vol. 30, pp. 767–782, Nov. 2020.
- [16] X. Li, Y. He, J. A. Zhang, and X. Jing, "Supervised domain adaptation for few-shot radar-based human activity recognition," *IEEE Sensors Journal*, vol. 21, no. 22, pp. 25 880–25 890, Oct. 2021.
- [17] Y. Xu, J. Yang, Y. Zhou, Z. Chen, M. Wu, and X. Li, "Augmenting and aligning snippets for few-shot video domain adaptation," in *Proc. ICCV*, Oct. 2023, pp. 13 445–13 456.
- [18] S. Das *et al.*, "Toyota smarhome: Real-world activities of daily living," in *Proc. ICCV*, Oct. 2019, pp. 833–842.
- [19] H. Kuehne, H. Jhuang, E. Garrote, T. A. Poggio, and T. Serre, "HMDB: A large video database for human motion recognition," in *Proc. ICCV*, Nov. 2011, pp. 2556–2563.
- [20] K. Soomro, A. R. Zamir, and M. Shah, "UCF101: A dataset of 101 human actions classes from videos in the wild," *arXiv preprint arXiv:1212.0402*, 2012.
- [21] N. Xiao and L. Zhang, "Dynamic weighted learning for unsupervised domain adaptation," in *Proc. CVPR*, Jun. 2021, pp. 15 242–15 251.
- [22] M. Li, Y. Zhai, Y. Luo, P. Ge, and C. Ren, "Enhanced transport distance for unsupervised domain adaptation," in *Proc. CVPR*, Jun. 2020, pp. 13 933–13 941.
- [23] W. Chang, T. You, S. Seo, S. Kwak, and B. Han, "Domain-specific batch normalization for unsupervised domain adaptation," in *Proc. CVPR*, Jun. 2019, pp. 7354–7362.
- [24] C. Lee, T. Batra, M. H. Baig, and D. Ulbricht, "Sliced wasserstein discrepancy for unsupervised domain adaptation," in *Proc. CVPR*, Jun. 2019, pp. 10 285–10 295.
- [25] M. Long, Y. Cao, J. Wang, and M. I. Jordan, "Learning transferable features with deep adaptation networks," in *Proc. ICML*, vol. 37, Jul. 2015, pp. 97–105.
- [26] M. Long, H. Zhu, J. Wang, and M. I. Jordan, "Deep transfer learning with joint adaptation networks," in *Proc. ICML*, vol. 70, Aug. 2017, pp. 2208–2217.
- [27] V. G. T. da Costa *et al.*, "Dual-head contrastive domain adaptation for video action recognition," in *Proc. WACV*, Jan. 2022, pp. 2234–2243.
- [28] J. Li, W. Liu, Y. Zhou, J. Yu, D. Tao, and C. Xu, "Domain-invariant graph for adaptive semi-supervised domain adaptation," *TOMM*, vol. 18, no. 3, pp. 1–18, Mar. 2022.
- [29] S. Motiian, Q. Jones, S. M. Iranmanesh, and G. Doretto, "Few-shot adversarial domain adaptation," in *Proc. NeurIPS*, vol. 30, Dec. 2017, pp. 6670–6680.
- [30] T. Teshima, I. Sato, and M. Sugiyama, "Few-shot domain adaptation by causal mechanism transfer," in *Proc. ICML*, vol. 119, Jul. 2020, pp. 9458–9469.
- [31] T. Jing, H. Xia, J. Hamm, and Z. Ding, "Marginalized augmented few-shot domain adaptation," *TNNLS*, pp. 1–11, Apr. 2023.
- [32] S. Huang, W. Yang, L. Wang, L. Zhou, and M. Yang, "Few-shot unsupervised domain adaptation with image-to-class sparse similarity encoding," in *Proc. MM*, Jun. 2021, pp. 677–685.
- [33] G. Bertasius, H. Wang, and L. Torresani, "Is space-time attention all you need for video understanding?" in *Proc. ICML*, vol. 139, Jul. 2021, pp. 813–824.
- [34] J. Carreira and A. Zisserman, "Quo vadis, action recognition? A new model and the kinetics dataset," in *Proc. CVPR*, Jul. 2017, pp. 4724–4733.
- [35] S. Yang, L. Liu, and M. Xu, "Free lunch for few-shot learning: Distribution calibration," in *Proc. ICLR*, May. 2021.
- [36] K. Simonyan and A. Zisserman, "Two-stream convolutional networks for action recognition in videos," in *Proc. NeurIPS*, vol. 27, Dec. 2014, pp. 568–576.
- [37] L. Wang *et al.*, "Temporal segment networks: Towards good practices for deep action recognition," in *Proc. ECCV*, vol. 9912, Oct. 2016, pp. 20–36.
- [38] D. Tran, L. D. Bourdev, R. Fergus, L. Torresani, and M. Paluri, "Learning spatiotemporal features with 3D convolutional networks," in *Proc. ICCV*, Dec. 2015, pp. 4489–4497.
- [39] S. Xie, C. Sun, J. Huang, Z. Tu, and K. Murphy, "Rethinking spatiotemporal feature learning: Speed-accuracy trade-offs in video classification," in *Proc. ECCV*, vol. 11219, Sep. 2018, pp. 318–335.
- [40] C. Feichtenhofer, "X3D: Expanding architectures for efficient video recognition," in *Proc. CVPR*, Jun. 2020, pp. 200–210.
- [41] K. Peng, A. Roitberg, K. Yang, J. Zhang, and R. Stiefelhagen, "TransDARC: Transformer-based driver activity recognition with latent space feature calibration," in *Proc. IROS*, Oct. 2022, pp. 278–285.
- [42] C. Szegedy *et al.*, "Going deeper with convolutions," in *Proc. CVPR*, Jun. 2015, pp. 1–9.
- [43] H. Fan *et al.*, "Multiscale vision transformers," in *Proc. ICCV*, Oct. 2021, pp. 6804–6815.
- [44] Z. Liu *et al.*, "Video swin transformer," in *Proc. CVPR*, Jun. 2022, pp. 3192–3201.
- [45] K. He, X. Zhang, S. Ren, and J. Sun, "Deep residual learning for image recognition," in *Proc. CVPR*, Mar. 2016, pp. 770–778.
- [46] X. Cong, B. Yu, T. Liu, S. Cui, H. Tang, and B. Wang, "Inductive unsupervised domain adaptation for few-shot classification via clustering," in *Proc. ECML PKDD*, vol. 12458, Sep. 2020, pp. 624–639.
- [47] J. Zhang, J. Zhu, Y. Yang, W. Shi, C. Zhang, and H. Wang, "Knowledge-enhanced domain adaptation in few-shot relation classification," in *Proc. KDD*, Aug. 2021, pp. 2183–2191.
- [48] T. Perrett, A. Masullo, T. Burghardt, M. Mirmehdi, and D. Damen, "Temporal-relational CrossTransformers for few-shot action recognition," in *Proc. CVPR*, Jul. 2021, pp. 475–484.
- [49] X. Wang *et al.*, "Hybrid relation guided set matching for few-shot action recognition," in *Proc. CVPR*, Jun. 2022, pp. 19 916–19 925.
- [50] W. Kay *et al.*, "The kinetics human action video dataset," *arXiv preprint arXiv:1705.06950*, 2017.
- [51] J. Munro and D. Damen, "Multi-modal domain adaptation for fine-grained action recognition," in *Proc. CVPR*, Jun. 2020, pp. 119–129.
- [52] D. P. Kingma and J. Ba, "Adam: A method for stochastic optimization," in *Proc. ICLR*, May. 2015.
- [53] E. Tzeng, J. Hoffman, K. Saenko, and T. Darrell, "Adversarial discriminative domain adaptation," in *Proc. CVPR*, Jul. 2017, pp. 2962–2971.
- [54] D. Schneider, M. S. Sarfraz, A. Roitberg, and R. Stiefelhagen, "Pose-based contrastive learning for domain agnostic activity representations," in *Proc. CVPR*, Jun. 2022, pp. 3432–3442.
- [55] B. Zhou, A. Andonian, A. Oliva, and A. Torralba, "Temporal relational reasoning in videos," in *Proc. ECCV*, Sep. 2018, pp. 803–818.
- [56] L. Van der Maaten and G. Hinton, "Visualizing data using t-SNE," *JMLR*, vol. 9, no. 11, Aug. 2008.